1 **Solar photolytic ozonation for the removal of recalcitrant herbicides in river water**

2 Rafael R. Solís [*,a,b], Sonia Medina [a], Olga Gimeno [a,b], Fernando J. Beltrán [a,b]

3 [a]Departmento de Ingeniería Química y Química Física, Universidad de Extremadura,

4 Avda. Elvas s/n, 06006 Badajoz, Spain

5 [b]Instituto Universitario de Investigación del Agua, Cambio Climático y Sostenibilidad,

6 Universidad de Extremadura, Avda. Elvas s/n, 06006 Badajoz, Spain

7 *Correspondence to Rafael Rodríguez Solís, Departamento de Ingeniería Química y

8 Química Física, Universidad de Extremadura, Avda. Elvas s/n, 06006, Badajoz (Spain).

9 Email: rrodrig@unex.es

10 **Abstract**

11 Photolytic ozonation of a river water has been performed by means of simulated solar

12 radiation. The application of solar radiation, limiting the complete radiation spectrum

13 (300-800 nm) to 320-800 nm and 390-800 nm, during the aqueous ozone decomposition

14 has been assessed. A kinetic mechanism, including the influence of initiation,

15 promotion and scavenging substances has been proposed, successfully modeling the

16 experimental data. Radiation improves O_3 decomposition rate, as a promoter, being

17 higher if the complete UV-visible spectrum is applied. Also, pH positively influences

18 O_3 decomposition rate from pH=4 to 8.

19 Photolytic ozonation has been also proved to be effective in the removal of a mixture of

20 three pyridine herbicides, dissolved in the river matrix. Radiation filters (320 nm and

21 390 nm cut-off) and pH have been selected as the main variables of the study. The

22 enhanced oxidation rate registered when applying solar radiation and O_3 relays on the

23 higher formation of hydroxyl radicals, responsible for the oxidation of these

24 recalcitrant-to-ozone herbicides. Moreover, the estimated R_{CT} ratios confirmed the

minimal differences of applying radiation or not at increasing pH, what is due to the ability of hydroxide anion to catalyze the decomposition of O_3 into $HO^{\bullet}$. The mineralization of the photolytic ozonation process (300-800 nm) reached 60%, whatever the pH considered. The increase of pH minimizes the differences in mineralization between the two technologies, the single ozonation achieving 50% at alkaline pH.

Keywords: photolytic ozonation, solar radiation, pyridine herbicides, river water

1. INTRODUCTION

Recently, there has been an increasing interest in the effect of a great number of chemicals appearing into the environment, as a consequence of human activities. One such example is the water pollution due to the named as micro-pollutants of emerging concern, widely detected in diverse aqueous resources around the world [1-4]. The term pollutant of 'emerging concern' involves unregulated pollutants for which monitoring data need to be gathered for supporting purposes in future prioritization exercises. They are also classified as micro-pollutant because they are frequently found in aquatic environments at low concentration level, i.e. mg L^{-1} or µg L^{-1} [2, 3]. Although their concentration is too low to produce acute toxic effects, the consequences of their exposition are unknown in the long term. On account of the raised diversity and volume of chemicals used, water pollution levels have increased and become more complex. Therefore, conventional treatment of wastewater and potable water has turn out to be less efficient [5]. The inefficient elimination of these substances threatens the reuse of polluted water under a circular economy concept. Cause by that, the development of new techniques involving the removal of these substances is required.

The possibility of implementing chemical oxidation, e.g. Advanced Oxidation Processes (AOPs) combined or not with classical treatment, has generated wide interest in the research community [6]. One such example is the use of ozone. Ozone is an interesting and versatile oxidant widely used for treating aqueous pollutants. Ozone application in diverse AOPs has gained attention due to its high efficiency to produce $HO^{\bullet}$ radicals by catalysis, radiation, and photocatalysis or combined with other oxidants like H_2O_2 [7, 8]. AOPs present the advantage of being effective in the oxidation of toxic recalcitrant substances towards biological treatment. The joint of chemical and biological technologies seem to be a promising solution to those effluents that cannot be entirely treated by microorganisms alone.

Although there is much research about diverse strategies for developing AOP, the high cost of these technologies and the further recovering of catalysts, or the consumption of extra chemicals, like H_2O_2, has not been resolved yet. The use of radiation presents the disadvantage of energy costs, especially when artificial UV radiation sources are applied. For this reason, the use of solar radiation emerges as an attractive and environmentally friendly solution, since it is a free and endless source of energy.

The primary focus of this paper is on the study of the combination of solar radiation and ozone as a possible AOP for the oxidation of organic pollutants in a river water. Firstly, the influence of radiation on ozone decomposition has been explored. This aspect has been the subject of several works in absence of radiation. Although considerable research has focused on the aqueous ozone decomposition kinetics from reaction mechanisms [9], based on experimental facts; rather less attention has been paid to the influence of radiation in these mechanisms, especially related with solar radiation [10]. Hence, the present work extends to the study of solar photolytic

ozonation decomposition kinetics in a river water matrix. A simplified mechanism based on the one of Staehelin, Hoigné, and Bühler [11] has been applied, considering the presence of initiator, scavenger and promoter substances. The importance of these factors in the presence and absence of simulated solar radiation have also been investigated at different pHs.

Secondly, photolytic ozonation, using simulated solar radiation (300-800 nm) has been studied for the oxidation of aqueous organic pollutants. As model compounds, a mixture of three pyridine herbicides which react slowly with ozone [12] has been chosen. These organics have been selected based on their solubility, widespread use in agriculture, persistence and environmental fate [13]. These herbicides have been dissolved in the selected river water matrix. The research has tended to focus on the mineralization and depletion rate of the herbicides, studying the influence of pH and the use of radiation filters (320-800 nm and 390-800 nm).

2. EXPERIMENTAL

2.1. River water and chemicals

Superficial river water was collected from Guadiana River on its course through the city of Badajoz, Spain (Geographical coordinates: 38.881716, -6.981106). Water samples were passed through cellulose filters in order to remove particles in suspension (> 11 µm), stored at 4 ºC and characterized as received. Table 1 summarizes the main characterization parameters obtained.

1   **Table 1.** Characterization of river water

Parameter (units)	Main value
Total Organic Carbon, TOC (mg L^{-1})	8.3 ± 0.5
Inorganic Carbon, IC (mg L^{-1})	45.4 ± 0.7
Chloride (mg L^{-1})	68.1 ± 0.3
Sulphate (mg L^{-1})	72.0 ± 0.4
pH	8.25 ± 0.01
Conductivity (μS cm^{-1})	571 ± 3
Turbidity (NTU)	6.2 ± 0.2
Absorbance 254 nm (dimensionless)*	0.107 ± 0.002

2   *Measured with a quartz cuvette of 1cm length path

3   The three pyridine herbicides (clopyralid, CLO, CAS: 1702-17-6; picloram, PIC,

4   CAS: 1918-02-1; and triclopyr, TRI, CAS: 55335-06-3) were analytical standard grade

5   (>99%). Analytical standards and solutions for analysis were prepared with ultrapure

6   water from a Milli-Q® academic system (18.2 MΩ cm^{-1}). The rest of the chemicals

7   used were analytical grade and used as purchased. Acetonitrile for LC analysis was

8   HPLC-grade.

9   **2.2. Experimental setup and procedure**

10   Oxidation experiments were carried out in a Suntest CPS simulator (1500 W, air-

11   cooled Xe arc lamp) in which a 500 mL borosilicate reactor, magnetically stirred, was

12   placed. Simulated solar spectrum was limited to 300-800 nm range by using a quartz

13   glass plus a borosilicated glass. Moreover, radiation was restricted to wavelengths over

14   to 320 nm and 390 nm by means of fixing two filters (Unipapel and Edmund Optics,

15   respectively). The radiation spectra of the simulated solar radiation in absence and

16   presence of the two studied filters are displayed in Figure S1. Ozone was generated in

17   an Anseros COM device and gaseous ozone concentration was monitored in an Anseros

18   GM-OEM and GM-PRO apparatus. Figure 1 depicts a scheme of the experimental

19   setup.

1   Batch experiments for the kinetic decomposition of ozone were carried out by

2   reaching saturation of dissolved ozone. After that, the solar simulator was switched on

3   in the presence or absence of the aforementioned filters. The experiment done in

4   absence of radiation, that means darkness, was performed by covering the reactor with

5   aluminum foil with the goal of maintaining similar temperature profiles for comparison

6   purposes. Semi-batch trials were carried by feeding ozone and radiation at the same

7   time. In both cases, at different times, samples were extracted for the aqueous analyses.

8   The experiments of degradation of the three selected pyridine-based herbicides were

9   carried out in semi-batch mode at initial concentration of 1 mg L^{-1} each.
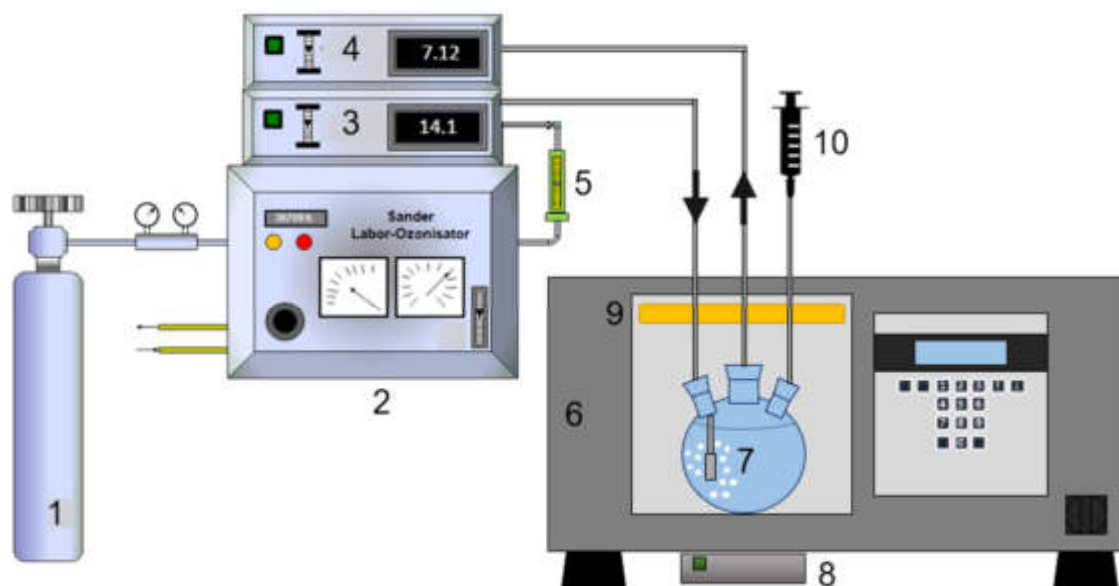
10

11   **Figure 1.** Experimental set-put scheme. 1: Oxygen tank; 2: Ozone Generator; 3: inlet

12   ozone analyzer; 4: outlet ozone analyzer; 5: flowrate meter; 6: simulated solar radiation

13   apparatus; 7: borosilicate glass reactor; 8: magnetic stirrer; 9: Xe arc lamp; 10: sampling

14

15   **2.3. Analytical methods**

16   The analysis of the three aqueous herbicides at an initial concentration of 1 mg L^{-1}

17   was carried out by means of HPLC with UV detection in an Agilent 1100 apparatus.

18   The stationary phase used was a Kromasil 100 5C18 (5 µm, 2.1 x 150 mm) column. A

50:50 (v/v) mixture of 0.1% H_3PO_4 acidified water and acetonitrile was pumped at a rate of 1 mL min^{-1}, obtaining retention times of 7.6, 9.5 and 16.9 min for clopyralid, picloram, and triclopyr, respectively. UV detection was conducted at 230 nm.

Total Organic Carbon (TOC) and Inorganic Carbon (IC) were analyzed in a Shimadzu TOC-V$_{CSH}$ device equipped with automatic sample injection.

Inorganic anions were analyzed by ion chromatography coupled to conductivity detector in a Methrom® 881 compact IC pro equipped with chemical suppression. The stationary phase was a MetroSepA Supp 5 column (250 x 4.0 mm, 5 μm), thermally controlled at 45 ºC. The mobile phase program consisted of a 0.7 mL min^{-1} gradient of Na_2CO_3 solution from 0.6 mM to 14.6 mM in 50 min.

Dissolved ozone concentration in aqueous solution was analyzed following the spectrophotometric method of indigo trisulfonate decoloration [14]. The generated hydrogen peroxide was quantified by the colorimetric method proposed by Masschelein and co-workers [15].

pH was measured in a GLP 21+ Crison® pH-meter equipped with a 50 21T electrode and conductivity in a Crison® 524 conductimeter device. Turbidity was measured in a 2100 IS Hach® turbidimeter.

3. RESULTS AND DISCUSSION

3.1. Ozone decomposition in presence of solar radiation.

3.1.1. *Pseudo-first order rate constants and pH influence*

In an attempt of study of the rate of ozone decomposition in the river water matrix, a series of experiments were carried out in order to compare the presence of solar radiation and the influence of visible and ultraviolet range at different pHs. Some experiments at pH=4, pH=6, and pH=8 were conducted for that purpose. In all of them,

after pH adjustment when necessary, the water sample was saturated with ozone at a

rate of 0.45 g h^{-1} until a constant value of dissolved ozone concentration was reached.

Next, ozone feeding was interrupted, and the rate of decomposition was studied in the

presence or absence of radiation. Figure 2 shows the evolution of normalized dissolved

ozone concentration during the decomposition stage. From Figure S2, on the other hand,

as example, saturation and ozone decomposition curves at pH 4 are depicted. As a mere

tool for comparison, the pseudo-first order rate constant of ozone decomposition, k', in

each situation was calculated. Table 2 summarizes the k' values and the regression

correlation calculated, which were in almost all cases fitted with $R^2 > 0.99$.

Table 2. Pseudo-first order rate constant (k', min^{-1}) of dissolved ozone decomposition

in presence and absence of radiation in the river water matrix. Influence of pH and

filters

System	pH=4		pH=6		pH=8	
	k'±error (min^{-1})	R^2	k'±error (min^{-1})	R^2	k'±error (min^{-1})	R^2
Darkness	0.026±0.001	0.996	0.037±0.002	0.997	0.12±0.01	0.998
SR (300-800 nm)	0.081±0.004	0.991	0.075±0.003	0.996	0.28±0.03	0.995
SR (320-800 nm)	0.085±0.004	0.993	0.078±0.007	0.991	0.24±0.03	0.990
vis-SR (390-800 nm)	0.062±0.005	0.983	0.075±0.005	0.993	0.23±0.01	0.999

As it can be observed from Figure 2, the presence of simulated solar radiation (SR)

results positive in the rate of decomposition of ozone, if compared to those carried out

in darkness. In order to avoid the influence of the temperature when adding radiation,

the experiment in absence of SR was carried out covering the reactor with aluminum

foil, avoiding the penetration of radiation into the solution. pH exerts a positive effect in

the increase of the rate of decomposition (k') since the presence of hydroxide anions

catalyzes ozone decomposition to lead the formation of the hydroperoxide anion [16-

18]. The k' values appreciated for the experiments at pH=4 match with those obtained by Chávez et al. [10] in ultrapure water, probably due to the removal of inorganic carbon content after pH decrease. The presence of radiation increases 3.16 folder the k' value at pH=4 while at pH=6 and pH=8 this value is just 2.01 and 2.39 folder, respectively. The higher the pH, the lesser the radiation influences due to the presence of hydroxide anions in solution. The no significant difference of k' when cut-off filters of 320 and 390 nm (spectra of 320-800 nm and 390-800 nm, respectively) were used, may indicate that the main contribution for ozone decomposition comes from visible radiation. The presence of dissolved organic matter may contribute to the decomposition of ozone [19], explaining the lack of difference in the three radiation systems applied. In this sense, an experiment of photolysis of the river water matrix was conducted (Figure S3), not being changes detected in the UV-vis spectrum in presence of the complete simulated solar radiation (300-800 nm). Otherwise, the lower values of k' at pH=8 if compared to what expected for ultrapure water [10] could be due to the presence of dissolved organic matter, the inorganic content and other impurities, which highly affect to ozone decomposition rate at this pH level [20].
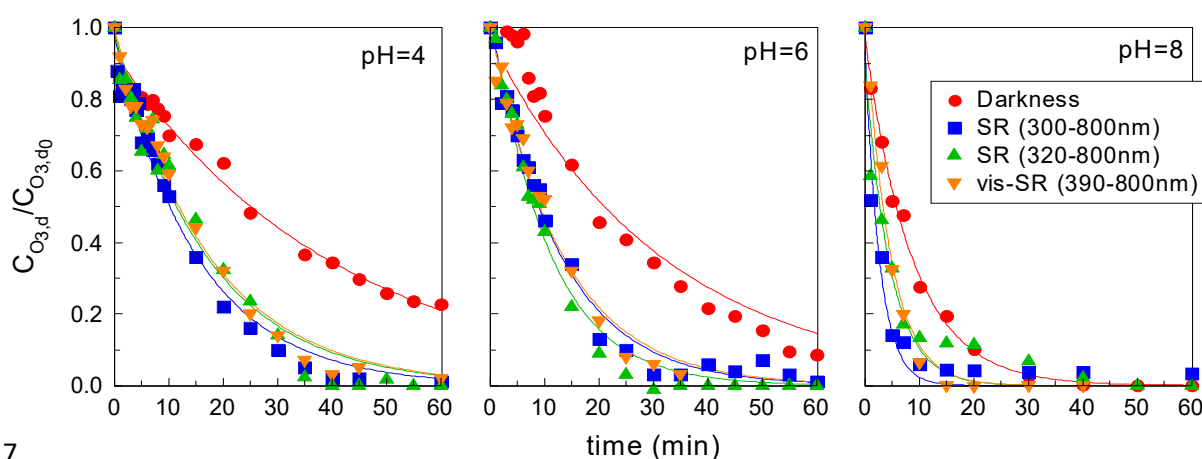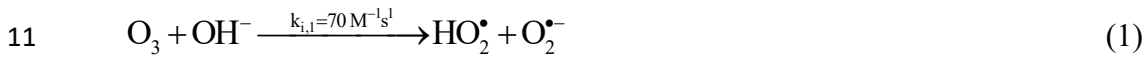
1 **Figure 2.** Ozone decomposition in the presence of solar radiation. Influence of radiation

2 cut-off filters and pH. Experimental conditions: V=500 mL; $C_{O3,d0}$=2.5-3.8 mg L^{-1}.

3 Symbols mean experimental data and straight lines the pseudo-first order fitting.

4

5 *3.1.2. Kinetic model approach*

6 Much research has been focused on the kinetics of ozone decomposition in water [9];

7 however, no kinetic studies have been developed in presence of radiation for a river

8 water matrix. For the kinetic approach proposed for this system, the mechanism

9 proposed by Staehelin, Hoigné, and Bühler [11] has been considered. The reactions of

10 ozone in water can be summarized in the followings:

11
$$O_3 + OH^- \xrightarrow{k_{i,1}=70\,M^{-1}s^{-1}} HO_2^{\bullet} + O_2^{\bullet-} \qquad (1)$$

12
$$HO_2^{\bullet} \underset{}{\overset{pKa=4.8}{\rightleftharpoons}} H^+ + O_2^{\bullet-} \qquad (2)$$

13
$$O_3 + OH^- \xrightarrow{40\,M^{-1}s^{-1}} HO_2^- + O_2 \qquad (3)$$

14
$$O_3 + HO_2^- \longrightarrow O_3^{\bullet-} + HO_2^{\bullet} \qquad (4)$$

15
$$O_3 + O_2^{\bullet-} \xrightarrow{k_1} O_3^{\bullet-} + O_2 \qquad (5)$$

16
$$O_3 + H^+ \xrightarrow{k_2} ... \rightarrow HO^{\bullet} + O_2 \qquad (6)$$

17
$$O_3 + HO^{\bullet} \xrightarrow{k_3=2\times10^9\,M^{-1}s^{-1}} HO_4^{\bullet} \qquad (7)$$

18
$$HO_4^{\bullet} \xrightarrow{2.8\times10^4\,M^{-1}s^{-1}} HO_2^{\bullet} + O_2 \qquad (8)$$

19 In a real water matrix, the presence of initiators, promoters, and inhibitors

20 extensively modify the kinetics of O_3 decomposition. The unknown nature and

21 concentration of these substances make difficult their inclusion in a kinetic model. For

22 that reason, they are included as a global term. Initiators (I), mainly organic compounds

23 that accelerate the reaction of ozone to produce $O_3^{\bullet-}$ radicals, can be included in the

1   kinetic model [21]. For simplification, only reactions that produce $O_3^{\bullet-}$ are considered.

2   The possible formation of $O_2^{\bullet-}$ or H_2O_2 is not included.

3     $$O_3 + I \xrightarrow{\;k_I\;} O_3^{\bullet-} \tag{9}$$

4   In the same way, promoter (P) and scavenger (S) substances consume $HO^{\bullet}$:

5     $$HO^{\bullet} + P \xrightarrow{\;k_P\;} HO_2^{\bullet} K \tag{10}$$

6     $$HO^{\bullet} + S \xrightarrow{\;k_S\;} End \tag{11}$$

7   The O_3 decomposition rate could be summarized to:

8     $$-r_{O_3} = k_{i,1} C_{O_3} C_{OH^-} + k_1 C_{O_2^{\bullet-}} C_{O_3} + k_3 C_{HO^{\bullet}} C_{O_3} + k_I C_I C_{O_3} \tag{12}$$

9   A steady-state balance of $O_2^{\bullet-}$ or $HO^{\bullet}$ leads to equations (13) and (14), respectively:

10     $$k_1 C_{O_2^{\bullet-}} C_{O_3} = 2k_{i,1} C_{OH^-} C_{O_3} + k_P C_P C_{HO^{\bullet}} + k_3 C_{HO^{\bullet}} C_{O_3} \tag{13}$$

11     $$k_1 C_{O_2^{\bullet-}} C_{O_3} + k_I C_I C_{O_3} = k_3 C_{HO^{\bullet}} C_{O_3} + k_P C_P C_{HO^{\bullet}} + k_S C_S C_{HO^{\bullet}} \tag{14}$$

12   Combining equations (12) and (13):

13     $$-r_{O_3} = 3k_{i,1} C_{O_3} C_{OH^-} + k_P C_P C_{HO^{\bullet}} + 2k_3 C_{O_3} C_{HO^{\bullet}} + k_I C_I C_{O_3} \tag{15}$$

14   The transient steady-state $C_{HO^{\bullet}}$ is obtained by substituting equation (13) into (14) and

15   solving $C_{HO^{\bullet}}$:

16     $$C_{HO^{\bullet}} = \frac{2k_{i,1} C_{O_3} C_{OH^-} + k_I C_I C_{O_3}}{k_S C_S} \tag{16}$$

17   The substitution of $C_{HO^{\bullet}}$ in equation (15) leads to the following equation, for a batch

18   reactor:

19     $$-r_{O_3} = -\frac{dC_{O_3}}{dt} = k_A C_{O_3} + k_B C_{O_3}^2 \tag{17}$$

20   where:

1

$$
\left. \begin{array}{l}
k_A = 3k_{i,1} + F_I + \dfrac{2k_{i,1}C_{OH^-} + F_P + F_I F_P}{F_S} \\[3mm]
k_B = \dfrac{4k_{i,1}k_3 C_{OH^-} + 2k_3 F_I}{F_S}
\end{array} \right\}
\tag{18}
$$

2   Being $F_I=k_I C_I$, $F_P=k_P C_P$ and $F_S=k_S C_S$ the initiator, promoter and scavenger factors.

3   At pH<4.8, $O_2^{\bullet-}$ is not produced from $HO_2^{\bullet}$ equilibrium. The differential equation

4   obtained for O_3 decomposition is the same as equation (17), but the balance of $O_2^{\bullet-}$ leads

5   to: $k_I C_{O_3} C_{O_2^{\bullet-}} = k_{i,1} C_{O_3} C_{OH^-}$. In this case, k_A and k_B are the followings:

6

$$
\left. \begin{array}{l}
k_A = F_I \\[3mm]
k_B = k_3 \dfrac{F_I}{F_S}
\end{array} \right\}
\tag{19}
$$

7   By adjusting the experimental data of C_{O3} vs time to the numerically resolved

8   differential equation (17), is possible to obtain the initiator, promoter and scavenger

9   factors from the k_A and k_B values.

10   Table 3 shows the values calculated for k_A and k_B after resolving equation (17) with

11   acceptable regression coefficients for the non-linear regression. Values of k_A can be

12   considered a first approximation to a 'pseudo-first order constant', previously

13   calculated, and the same conclusions can be extracted for the comparison in between the

14   systems and the considered pHs.

15   **Table 3.** k_A (s^{-1}) and k_B (M^{-1}s^{-1}) values calculated for the kinetic model of ozone

16   decomposition, equation (17). Influence of pH and filters

System	pH=4			pH=6			pH=8		
	$k_A \cdot 10^3$	$k_B \cdot 10^7$	R^2	$k_A \cdot 10^3$	$k_B \cdot 10^7$	R^2	$k_A \cdot 10^3$	$k_B \cdot 10^7$	R^2
Darkness	0.44	1.70	0.994	0.53	0.54	0.987	1.75	1.72	0.991
SR (300-800 nm)	1.12	3.80	0.993	1.28	2.53	0.988	4.80	2.54	0.956
SR (320-800 nm)	1.36	1.83	0.992	1.44	1.70	0.987	3.42	1.57	0.960
vis-SR (390-800 nm)	1.02	1.72	0.985	1.28	2.32	0.989	2.94	1.46	0.992

17

Figure 3 shows the initiator, promoter and scavenger factors calculated from k_A and k_B values of Table 3 for each system at the three pHs studied. From equation (19) is possible to calculate initiation and scavenger factors at acidic conditions. Moreover, since the media contains inorganic carbon at pHs 6 and 8, the scavenger factor due to these species can be calculated taking into account the reaction of carbonate and bicarbonate with hydroxyl radicals [22]:

$$HO^{\bullet} + HCO_3^- \xrightarrow{\ k_{c1}=8.5\,10^6\,M^{-1}s^{-1}\ } CO_3^{\bullet-} + H_2O \tag{20}$$

$$HO^{\bullet} + CO_3^{2-} \xrightarrow{\ k_{c1}=3.9\,10^8\,M^{-1}s^{-1}\ } CO_3^{\bullet-} + HO^- \tag{21}$$
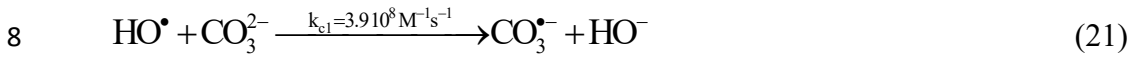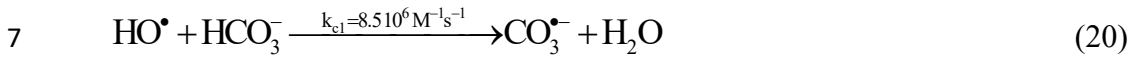
The scavenger factor due to the presence of alkalinity can be determined as follows [9]:

$$k_t = k_{c1}C_{HCO_3^-} + k_{c2}C_{CO_3^{2-}} = \left(k_{c1} + k_{c2}10^{pH-pK_2}\right)\frac{10^{pH-pK_1}}{1+10^{pH-pK_1}+10^{2pH-pK_1-pK_2}}C_{HCO_3^-,t}$$

$$\tag{22}$$

Where $pK_1=6.35$ and $pK_2=10.33$ are the pK_a equilibrium of carbonates in water, and $C_{HCO_3^-,t}$ the concentration of inorganic carbon expressed as HCO_3^-. At pH=6 k_t was calculated to be $6.34 \cdot 10^9$ $M^{-1}s^{-1}$, and at pH=8 it was $7.79 \cdot 10^9$ $M^{-1}s^{-1}$. These values are 10^3 inferiors to the calculated from the proposed kinetic model (in the range of 10^{12} $M^{-1}s^{-1}$). This likely means that the scavenger effect of alkalinity is less important than the one due to the rest of substances present in the water matrix, that probably react with $HO^{\bullet}$ if compared to reactions (20) and (21). These results would explain why no differences of F_S with pH are appreciated.

F_I and F_p were calculated from equation (18) at pH>4.8. F_I is higher in presence of radiation and acidic conditions. F_P also increases if water is irradiated; however, this aspect is only appreciated at alkaline conditions.
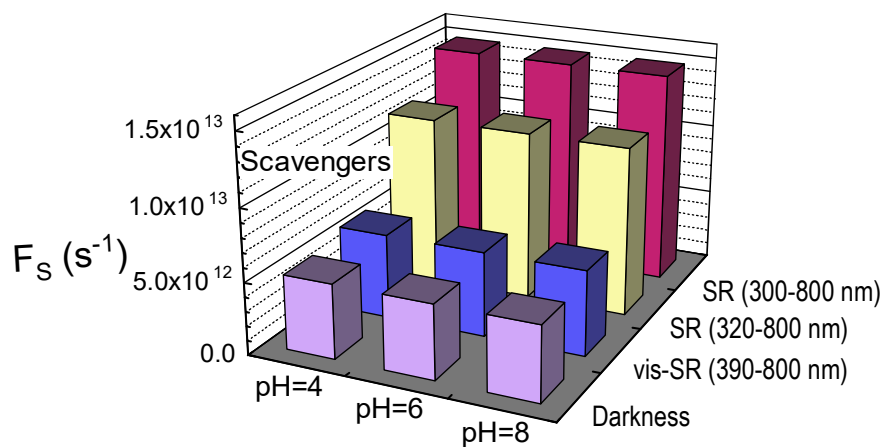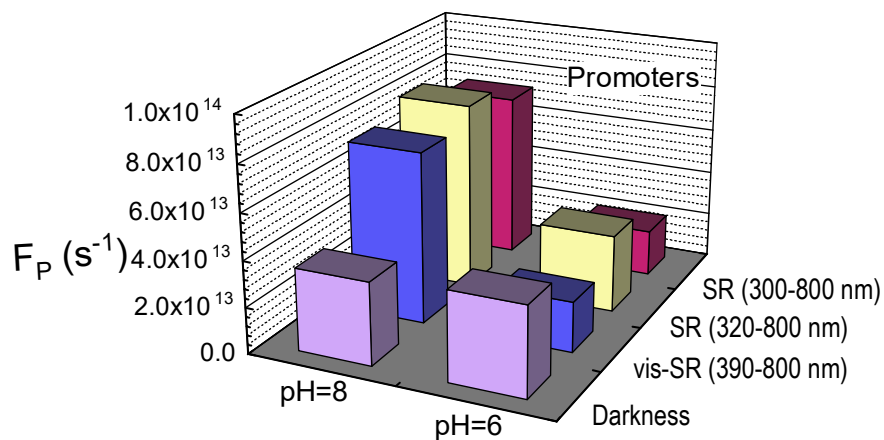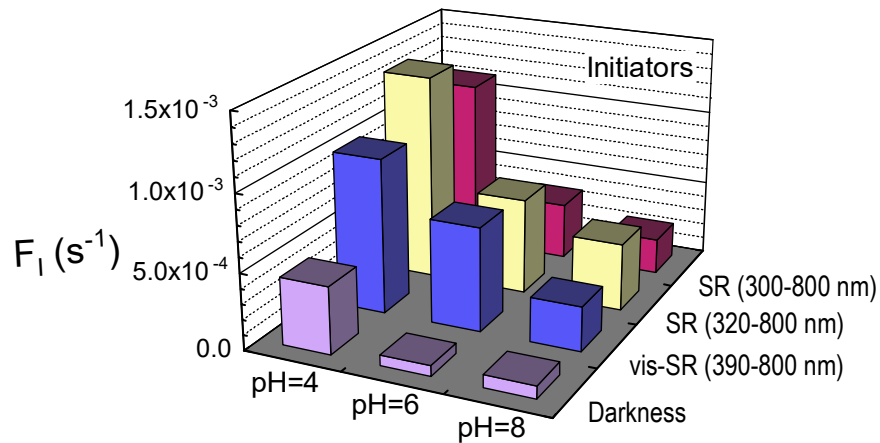
Figure 3. Initiation (I), scavenger (S) and promoter (P) factors during O_3 decomposition in the river water. Influence of pH, the presence of solar radiation (SR) and filters
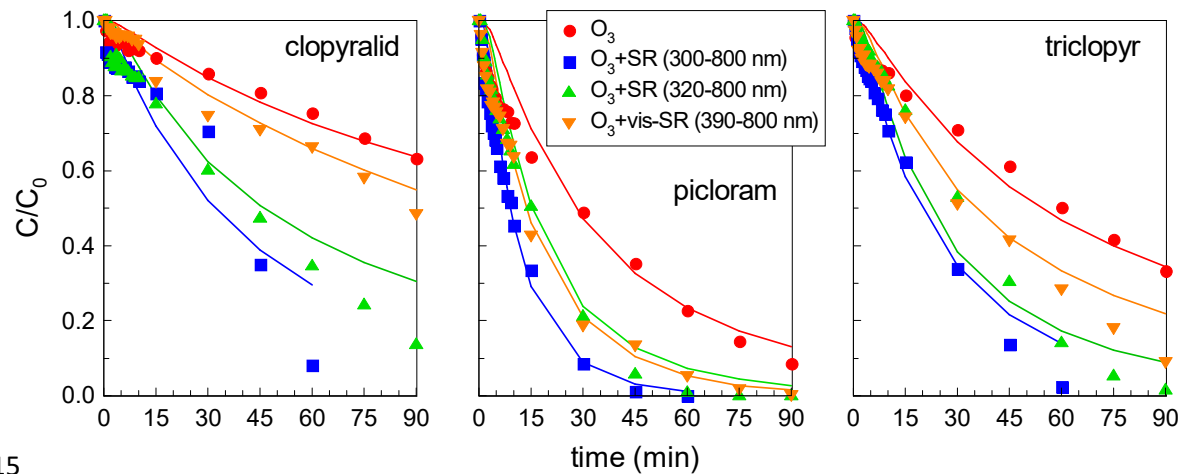
1 **3.2. Photolytic ozonation of herbicides in river water matrix**

2 The combination of ozone and solar radiation was also assessed in the removal of a

3 mixture of three pyridine-based herbicides as model aqueous organic pollutants. For

4 reaching that purpose, 1 mg L^{-1} of each herbicide (clopyralid, picloram an triclopyr) was

5 added to the river water and pH was adjusted when required.

6

7 *3.2.1.pH and radiation filters influence in removal efficiency of herbicides*

8 As studied previously, pH and the radiation nature, i.e. its restriction using filters,

9 was considered as the most important variables in this study. Thus, a series of

10 experiments were conducted comparing the behavior of photolytic ozonation and ozone

11 in the oxidation rate of the mixture of the three herbicides. Figure 4 depicts the

12 dimensionless remaining concentration of herbicides versus time for a period of 90 min

13 photolytic ozonation at pH=4. The results at pH=6 and pH=8 (the natural pH of the river

14 water) are shown in Figure S4.

16 **Figure 4.** Photolytic ozonation of the pyridine-based herbicides at pH=4. Influence of

17 radiation filters in the herbicides' removal. Experimental conditions: V=500 mL;

18 $C_{O3,inlet}$=15 mg L^{-1}; Q_{GAS}=30 L h^{-1}; $C_{herb,0}$=1 mg L^{-1}, pH=4 (buffered with 10 mM of

1   H_3PO_4). Symbols represent experimental data and the straight lines the simulation

2   through the calculated R_{CT} values

3

4   Figure 4 reveals some interesting results about the effect of radiation during the

5   ozonation process. According to the results, the reactivity order appreciated is

6   picloram>triclopyr>clopyralid which matches the reported second order rate constant

7   with ozone (k_{O3}) in literature. For clopyralid and triclopyr, k_{O3} is reported to be 0.3 $M^{-1} \cdot s^{-1}$ [12]; whereas for picloram the following values are published: 0.8 $M^{-1} \cdot s^{-1}$ [23], 2.3

9     $M^{-1} \cdot s^{-1}$ [24] and 1.75 $M^{-1} \cdot s^{-1}$ [12]. The high recalcitrance to direct reaction with ozone

10   makes the radical pathway to play the main oxidation route.

11   Solar radiation enhances the decomposition of ozone into hydroxyl radicals [10],

12   accelerating the removal rate of the herbicides as shown in Figure 4. The oxidation rate

13   is improved if all the solar simulated spectrum is applied (300-800 nm). For example,

14   under acidic conditions, photolytic ozonation with all the spectrum achieves a complete

15   degradation in 60-90 min depending on the herbicide, while after 90 min of single

16   ozonation an important amount of the most recalcitrant remains (>60% of clopyralid

17   and >30% of triclopyr). If the spectrum is limited to 320 nm or 390 nm (visible range),

18   the enhancement of the oxidation rate is more limited, the visible being the less

19   effective. At pH=6 and 8 (see Figure S4), the oxidation times required for a complete

20   oxidation of the three herbicides are shortened. This effect can be attributed to the

21   catalytic effect of hydroxide anions in the decomposition of ozone into hydroxyl

22   radicals. Therefore, due to this fact, the addition of radiation as a radical promoter lacks

23   importance and the enhancement observed in the removal rate of the compounds is

24   minimal.

To quantify the removal rates, and just as a mere comparison tool, Figure 5 depicts the observed pseudo-first order rate constants (k', $R^2 > 0.99$) for each herbicide under the studied oxidation systems at pHs 4, 6 and 8. As inferred in this figure, the presence of solar simulated radiation exerts a positive effect, especially under acidic conditions. At pH=6, and at pH=8 also, the increase of k'-values registered after addition of radiation is more restricted. The benefit of O_3+SR (300-800 nm) if compared to O_3+SR (320-800 nm) appreciated at pH=4, is negligible at higher pHs. Finally, it is worth to highlight that the pH effect prevails in the application of radiation as a radical promoter.
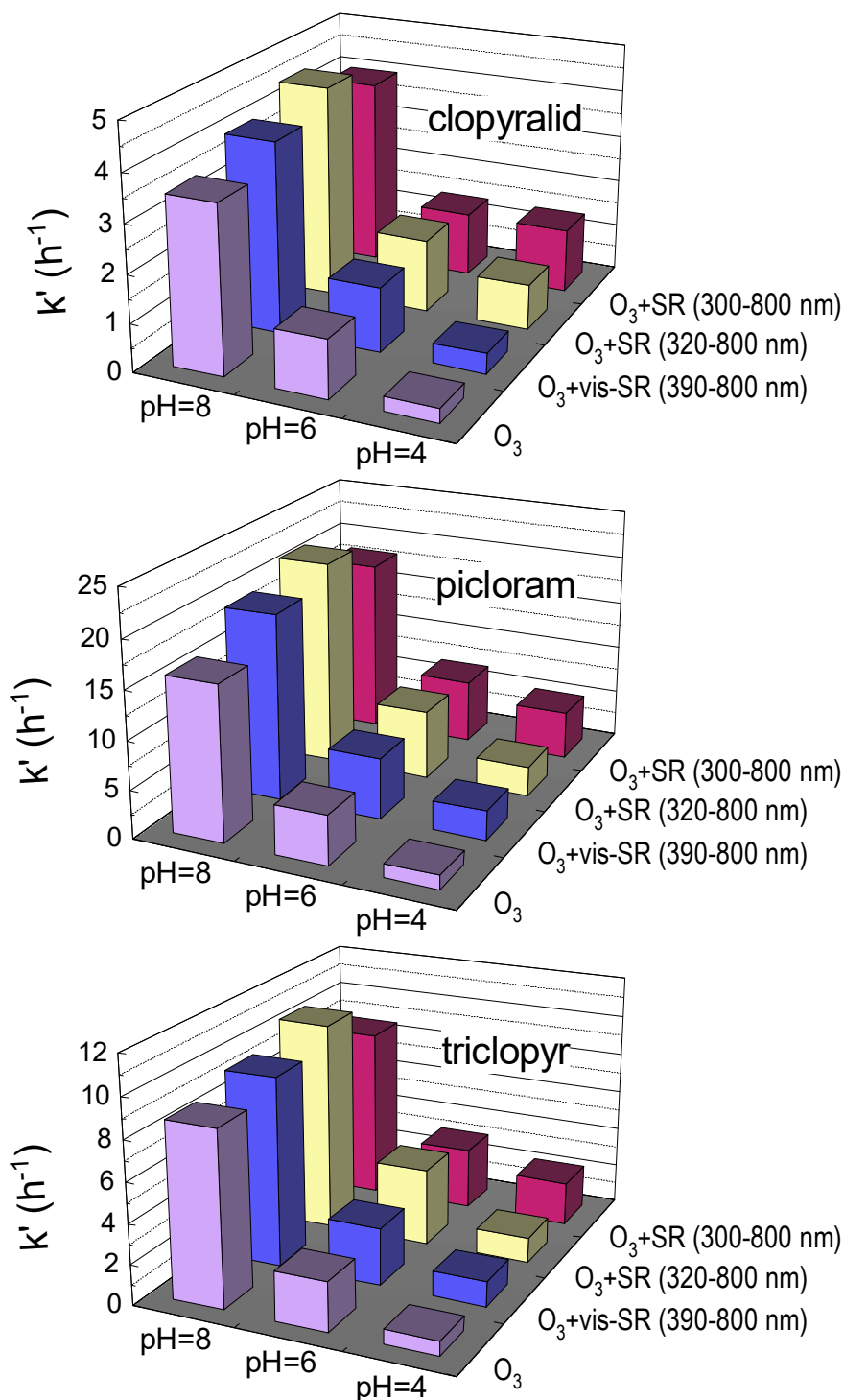
Figure 5. Photolytic ozonation of the pyridine-based herbicides. Influence of pH and radiation filters on the pseudo-first order rate constant (k'). Experimental conditions: V=500 mL; $C_{O3,inlet}$=15 mg L^{-1}; Q_{GAS}=30 L h^{-1}; $C_{herb,0}$=1 mg L^{-1}, pH=4 and 6 (buffered with 10 mM of H_3PO_4) and pH=8 (non-buffered)

1

3.2.2. Influence of radiation on R_{CT} ratios and radical pathway

The hydroxyl radical production can be evaluated through the R_{CT} concept [25]. R_{CT} is defined as the ratio of HO• to ozone exposure and is frequently used as an indirect tool to measure HO• concentration:

$$R_{CT} = \frac{C_{HO\bullet}}{C_{O_3}} = \frac{\int_0^t C_{HO\bullet} dt}{\int_0^t C_{O_3} dt} \qquad (23)$$

Considering the second-order for the reaction between O_3 or HO• and the herbicide, first-order in both O_3 or HO• and the compound, the kinetic expression of the depletion of the herbicide (i) in a batch reactor can be described as:

$$-r_i = \frac{dC_i}{dt} = k_{O_3,i} C_{O_3} C_i + k_{HO\bullet,i} C_{HO\bullet} C_i \qquad (24)$$

where $k_{O3,i}$ and $k_{HO\bullet,i}$ are the second order rate constants of the reactions between the herbicide and O_3 or HO•, respectively. After integration and inclusion of R_{CT} concept, the equation (24) leads to the following [26]:

$$\ln\frac{C_{i_0}}{C_i} = \left(k_{O_3,i} + k_{HO\bullet,i} R_{CT}\right) \int_0^t C_{O_3} dt \qquad (25)$$

A linear representation of the logarithmic term versus the dissolved ozone exposure conducts to a straight line whose slope allows the R_{CT} value to be obtained. This parameter can be easily quantified since the dissolved ozone concentration was monitored with time (Figure S5). For $k_{O3,i}$ and $k_{HO\bullet,i}$, the reported values by Solís et al. [12] were considered. Accordingly, the R_{CT} values for each herbicide at the different situations of pH and radiation applied ($R^2 > 0.99$) were determined. Under the same

19

1   conditions of pH and radiation, the R_{CT} values individually calculated for each herbicide

2   were quite similar, and the media of the three values was taken. These values are shown

3   in Figure 6. The trend appreciated explains the behavior already appreciated in the

4   herbicides removal rate. The presence of radiation enhances the production of hydroxyl

5   radicals. For example, in the simultaneous application of the complete SR spectrum and

6   ozone leads to *circa* 5-fold the R_{CT} value if compared to single ozonation at pH=4. At

7   higher pH, this increase is less pronounced (*ca.* 1.5 and 2.33-fold at pH=6 and 8,

8   respectively). Nevertheless, the effect of pH is more important than the addition of

9   radiation. For example, R_{CT} value is increased approximately 14 times from pH=4 to 8

10   (for single ozonation).

11   Figure 4 also depicts the simulated profiles of each herbicides oxidation according to

12   the calculated R_{CT} ratios. As can be appreciated, R_{CT} is a valuable tool for fitting the

13   experimental results, especially at the initial reaction times. As reaction progresses,

14   some intermediates are triggered. Therefore, these species compete with the initial

15   compounds during the reaction with HO$^{\bullet}$. That is the reason why at long times the

16   simulated profiles via R_{CT} deviate from experimental data.

17
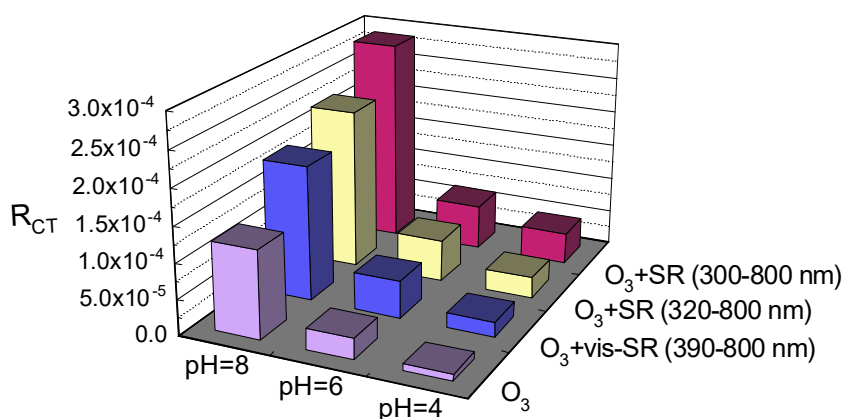
Figure 6. Photolytic ozonation of the pyridine-based herbicides. Influence of pH and radiation filters in the hydroxyl radical-dissolved ozone ratio, R_{CT}. Experimental conditions as shown in figure 5.

R_{CT} ratio is usually calculated with organic compounds which present a high recalcitrance towards ozone as probe-molecules, such as p-chlorobenzoic acid (pCBA) [25] or oxalic acid [10]; disregarding the direct reaction between ozone and the organic molecule. Although the direct reaction of the herbicides with ozone $k_{O3,i}$ is in the range of reactivity of the commonly used probe-molecules, it was also considered when calculating the R_{CT}. In order to corroborate the predominance of radical reaction, the contribution of the indirect or radical pathway ($\eta_{HO\bullet}$) has been assessed:

$$\eta_{HO\bullet} = \frac{r_{HO\bullet}}{r_{HO\bullet} + r_{O_3}} = \frac{k_{HO\bullet} C_{HO\bullet}}{k_{HO\bullet} C_{HO\bullet} + k_{O_3} C_{O_3}} \tag{24}$$

The evolution of the hydroxyl radical contribution with time at pH=4 is schematized in Figure 7. This ratio demonstrates the importance played by hydroxyl radical. Thus, only for clopyralid and picloram an appreciable contribution of the direct reaction with ozone (20%) is observed. The addition of solar radiation potentiates the radical pathway, the ratio $\eta_{HO\bullet}$ being increased to values >90%. In the case of clopyralid, where the differences between irradiated systems are more remarkable, a higher importance of radical pathway is revealed in the order SR (300-800 nm)>SR (320-800 nm)>vis-SR (390-800 nm). At pH=6 this ratio is >94%, and at pH=8 is >98%, regardless of the radiation applied (see Figure S6).
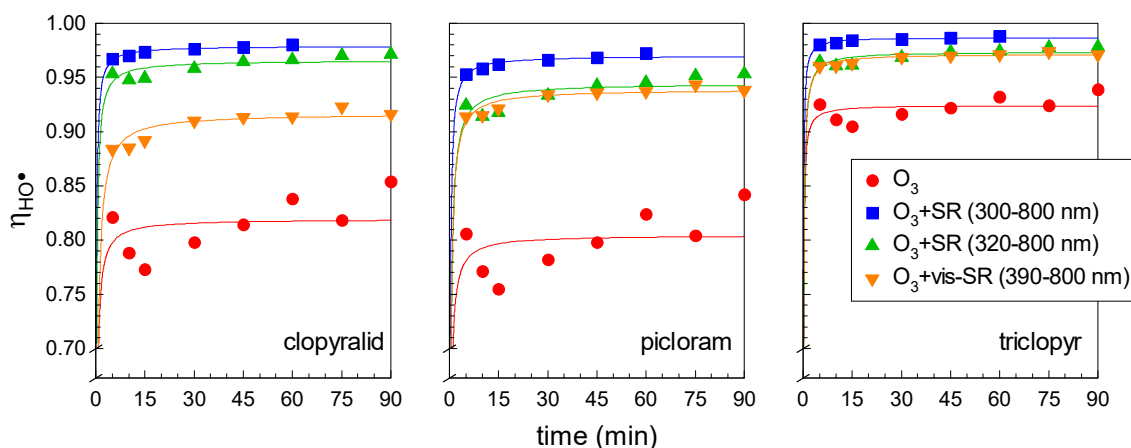
Figure 7. Photolytic ozonation of the pyridine-based herbicides. Influence of radiation filters on the evolution of the hydroxyl radical contribution ($\eta_{HO\bullet}$) at pH=4. Experimental conditions as shown in figure 4.

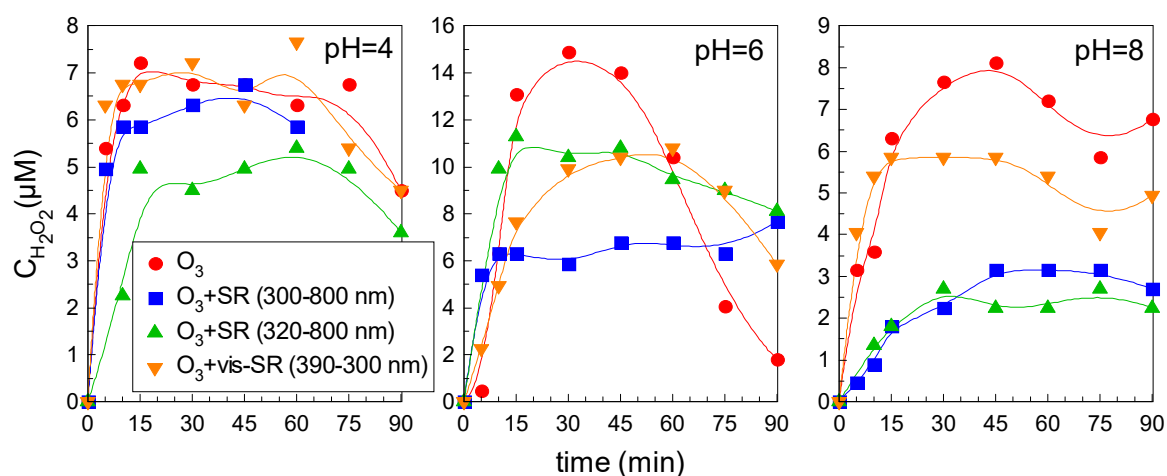### 3.2.3. Generated hydrogen peroxide in the photo-assisted ozonation

It is well documented that hydrogen peroxide is generated when ozone is applied in water during its indirect reaction pathway [11, 27]. Moreover, the ozonation of some organic also leads to the formation of H_2O_2 when ozone attacks aromatic rings, or carbon double bonds through the Criegee mechanism [28]. Furthermore, if radiation is included in the process, more H_2O_2 can be produced during the photolysis of ozone. Although ozone presents a maximum of radiation absorption at 254 nm, the spectrum of absorption is extended to 350 nm [29]. For that reason, H_2O_2 can be detected under aqueous ozonation irradiated with UV radiation [30] or solar radiation [10]:

$$O_3 + H_2O \xrightarrow{\ h\nu\ } O_2 + H_2O_2 \tag{25}$$

Hydrogen peroxide can undergo photolysis under UV radiation, yielding more HO$^\bullet$ radicals:

$$H_2O_2 \xrightarrow{\ h\nu\ } 2HO^\bullet \tag{26}$$

22
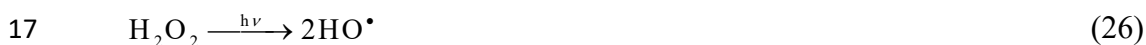
1 Nevertheless, the photolysis of hydrogen peroxide to produce two $HO^{\bullet}$ is disfavored due

2 to the higher molar extinction coefficient of O_3 if compared to H_2O_2. H_2O_2 photolysis

3 takes relevance when using radiation of wavelength lower than 320 nm [31]. Moreover,

4 this process can also take place with an alternative to artificial UV radiation source.

5 Actually, SR has been proved to be favorable from an economic and environmental

6 point of view in the activation of H_2O_2 [32].

Figure 8. Photolytic ozonation of the pyridine-based herbicides. Influence of pH and radiation filters on the evolution of the generated hydrogen peroxide. Experimental conditions as shown in figure 5.

11 Figure 8 shows the formation of hydrogen peroxide during the ozonation and SR

12 photolytic ozonation of the pyridine-based herbicides in the river water matrix at pH=4,

13 6 and 8. Under acidic conditions, similar profiles of generated H_2O_2 are registered, with

14 values in between 5 and 7 μM. At pH=6 a maximum of 15 μM of H_2O_2 is registered

15 under the ozonation process at 30 min, which is almost completely consumed after 90

16 min. Application of the less energetic radiations (320-800 nm and 390-800 nm) seem to

17 lead to maxima of 11 μM to slightly decrease while the most energetic conducts to a

18 steady-state concentration of H_2O_2. At pH=8, the photolytic ozonation with SR (300-

800 nm) and SR (320-800 nm) led to less production of H_2O_2 if compared to single

ozonation or vis-SR (390-800 nm) ozonation. At this pH, the higher concentration of

H_2O_2 registered during ozonation or visible photolytic ozonation can be attributed to a

lack of UV radiation that triggers H_2O_2 photolysis.

3.2.4. Aromaticity evolution and mineralization during photocatalytic ozonation

The benefit of radiation to promote the further oxidation of the intermediate and final

products was studied by monitoring the evolution of Total Organic Content (TOC) and

aromaticity. For that purpose, a series of trials with a higher concentration of the

herbicides were carried out (10 mg L^{-1} of each) and the mineralization degree was

assessed.

Absorbance at 254 nm (A_{254}) is usually measured as a general parameter indicative

of aromatic organic compounds presence in solution [9]. The absorbance registered for

the water matrix was 0.107. This value is augmented to 0.471 in the presence of the

pyridine-based herbicides. Therefore, the aromatic content of the water matrix

represents 23% of the total. Figure S7 depicts the evolution of the normalized evolution

of A_{254} with time during ozonation and photolytic ozonation at the three pH studied.

Pyridine-based herbicides, under HO•, are expected to undergo dechlorination and a fast

opening of the aromatic compound [33-37], leading to non-aromatic organic

compounds. Therefore, A_{254} may indicate the removal of the parent compound and the

first aromatic intermediates. Only at pH=4 differences of A_{254} removal with the SR

filters are appreciated. Single ozonation removes 70% of aromatic content in 2 h, while

photolytic ozonation leads to 90% when all SR spectrum is applied. Vis-SR photolytic

ozonation conducts to 80%. At pH=6 differences between the systems are minimal with

1 all of them leading to a 90% of aromaticity removal; and at alkaline conditions (pH=8)

2 all systems led to the same A_{254} profiles. The aforementioned behavior pattern and

3 explanation given for herbicides oxidation can be extrapolated on how radiation and pH

4 affect A_{254} evolution.

5 Figure 9 shows the results of mineralization attained at the three pHs studied. As

6 expected, negligible mineralization extent was achieved during single ozonation, except

7 for alkaline conditions, in which the presence of hydroxide anions catalyze the

8 formation of hydroxyl radicals. Ozonation is a powerful technology for oxidation of a

9 vast variety of organic micropollutants; however, its main drawback is related to the

10 low mineralization achieved [38] due to the formation of refractory intermediates [39]

11 or final carboxylic acids, hardly oxidizable [40, 41]. For that reason, the promotion of

12 the hydroxyl radical pathway is a useful tool to improve the mineralization extent. As

13 can be inferred from Figure 9, a 60% mineralization in 2 h is registered if solar radiation

14 (300-800 nm) is simultaneously applied during ozonation at pH=4 and 6. The

15 application of vis-SR (390-800 nm) did also enhance the mineralization degree, though

16 in a lesser extent (40% in 2 h). The UV region of the solar spectrum is more effective in

17 the oxidation of organic matter than the visible region [42].

18 Under alkaline conditions, the TOC removed almost reached maximum of 60%

19 observed when adding radiation. Furthermore, the application of radiation, whatever the

20 spectrum was, led to a 60% mineralization. This lack of differences between the

21 systems can be attributed to the catalytic effect of hydroxide anions in ozone

22 decomposition. Basically, ozonation under these conditions can be considered by itself

23 as an AOP, being unnecessary the presence of other reagents or agents.

24
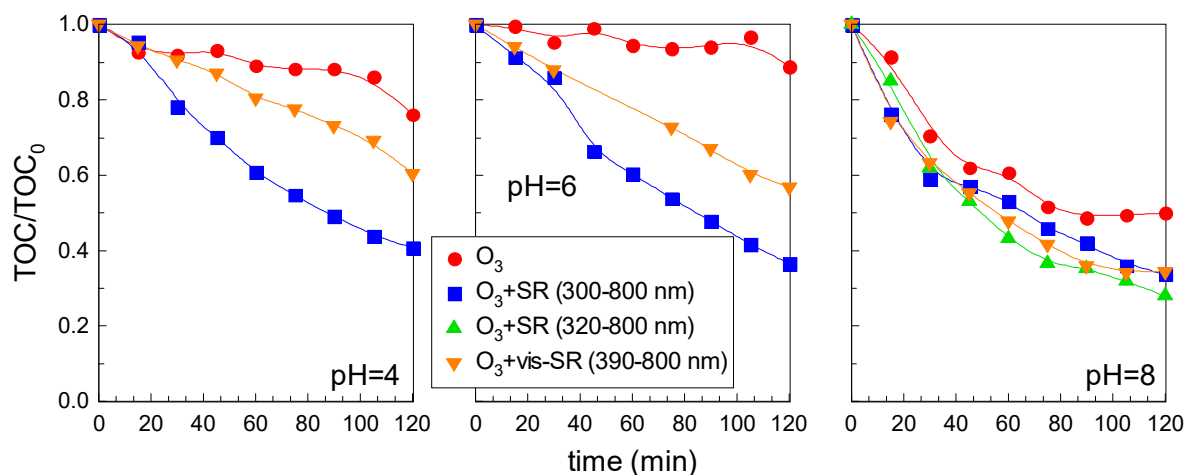
Figure 9. Photolytic ozonation of the pyridine-based herbicides. Influence of pH and radiation filters on the mineralization. Experimental conditions: V=500 mL; $C_{O3,inlet}$=15 mg L^{-1}; Q_{GAS}=30 L h^{-1}; $C_{herb,0}$=10 mg L^{-1}, TOC_0=17.6 mg L^{-1}; pH=4 or 6 (buffered with 10 mM of H_3PO_4) and pH=8 (non-buffered).

The mineralization reached during photolytic ozonation is linked to the ability of this technology to increase the formation of hydroxyl radicals as the previously calculated R_{CT} ratios proved. In contrast to ozone, HO$^{\bullet}$ do attack the final oxidation species generated in the oxidation of these herbicides, e.g. oxalic, formic and acetic acids [12]. This explains the enhancement of mineralization achieved in the presence of radiation or at increasing the pH.

CONCLUSIONS

The simultaneous application of ozone and solar radiation accelerates the O_3 decomposition rate of in a river water matrix. The initiation and promotion rates are improved in presence of UV-visible radiation, the first being promoted at acidic conditions while the second is favored at basic pH. Although radiation enhances the formation of HO$^{\bullet}$, the catalytic effect of hydroxide anion plays a more important role.

Consequently, photolytic ozonation as AOP mainly deserves attention under acidic conditions.

Photolytic ozonation is also an effective technology to treat refractory-to-ozone organic pollutants, increasing its effectiveness at acidic pHs. Meaningful enhance in the pseudo-first order rate constant was registered at pH=4 if radiation was applied. As pHs moves to the alkaline region, rate constant values increase regardless of radiation application. Mineralization followed similar behavior, reaching maxima of 60% at combining solar radiation and O_3, independently of the pH tested. The calculated R_{CT} ratios showed a higher concentration of $HO^\bullet$ in presence of radiation and/or increasing pH. Concretely, the raise of pH from 4 to 8 increased 14 times the production of $HO^\bullet$ during single ozonation; whereas the presence of solar radiation (300-800 nm) led to 5-folded R_{CT}. Moreover, under alkaline conditions, the addition of radiation does not enhance the result already achieved without radiation. This effect is attributed to the catalytic effect produced by hydroxide anions, which makes unnecessary the application of radiation to promote the formation of extra hydroxyl radicals.

Acknowledgments

References

[1] J.C.G. Sousa, A.R. Ribeiro, M.O. Barbosa, M.F.R. Pereira, A.M.T. Silva, A review on environmental monitoring of water organic pollutants identified by EU guidelines, J. Hazard. Mater. 344 (2018) 146-162. https://doi.org/10.1016/j.jhazmat.2017.09.058

[2] S.D. Richardson, T.A. Ternes, Water analysis: emerging contaminants and current issues, Anal. Chem. 90 (2018) 398-428. https://doi.org/10.1021/acs.analchem.7b04577

[3] V. Geissen H. Mol, E. Klumpp, G. Umlauf, M. Nadal, M. van der Ploeg, S.E.A.T.M. van de Zee, C.J. Ritsema, Emerging pollutants in the environment: A challenge for water resource management, Inter. Soil Water Conservation Res. 3 (2015) 57-65. https://doi.org/10.1016/j.iswcr.2015.03.002

[4] D.E. Vidal-Dorsch, S.M. Bay, K. Maruya, S.A. Snyder, R.A. Trenholm, B.J. Vanderford, contaminants of emerging concern in municipal wastewater effluents and marine receiving water, Environ. Toxicol. Chem. 31 (2012) 2674-2682. https://doi.org/10.1002/etc.2004

[5] K. Kümmerer, D.D. Dionysiou, O. Olsson, D. Fatta-Kassinos, A path to clean water, Sci. 361 (2018) 222-224. https://doi.org/10.1126/science.aau2405

[6] M. Salimi, A Esrafili, M. Gholami, A Jonidi Jafari, R. Rezaei Kalantary, M. Farzadkjia, M Kermani, H.R. Sobhi, Contaminants of emerging concern: a review of new approach in AOP technologies, Environ. Monit. Assess. 189 (2017) 414. https://doi.org/10.1007/s10661-017-6097-x

[7] S. Esplugas, D.M. Bila, L.G.T. Krause, M. Dezotti, Ozonation and advanced oxidation technologies to remove endocrine disrupting chemicals (EDCs) and pharmaceuticals and personal care products (PPCPs) in water effluents, J. Hazard. Mater. 149 (2007) 631-642. https://doi.org/10.1016/j.jhazmat.2007.07.073

[8] D. Robert, N. Keller, E. Selli, Environmental photocatalysis and photochemistry for a sustainable world: a big challenge, Environ. Sci. Pollut. Res. 24 (2017) 12503-12505. https://doi.org/10.1007/s11356-017-8935-3

[9] F.J. Beltrán, Ozone Reaction Kinetics for Water and Wastewater Systems, Lewis Publishers, Boca Ratón, 2004.

[10] A.M. Chávez, A. Rey, F.J. Beltrán, P.M, Álvarez, Solar photo-ozonation: A novel treatment method for the degradation of water pollutants, J. Hazard. Mater. 317 (2016) 36-43. https://doi.org/10.1016/j.jhazmat.2016.05.050

[11] R.E. Bühler, J. Staehelin, J. Hoigné, Ozone decomposition in water studied by pulse radiolysis. 1. Perohydroxyl (HO2)/hyperoxyde (O2-) and HO3/O3- as intermediates, J. Phys Chem. 88 (1984) 2560-2564. https://doi.org/10.1021/j150666a600

[12] R.R. Solís, F.J. Rivas, O. Gimeno, J.L. Pérez-Bote, Photocatalytic ozonation of clopyralid, picloram and triclopyr. Kinetic, toxicity and influence of operational parameters, J. Chem. Technol. Biotechnol. 91 (2016) 51-58. https://doi.org/10.1002/jctb.4542

[13] T.J. Monaco, S.C. Weller, F.M. Ashton, Weed Science. Principles and Practices, fourth ed., John Willey & Sons, New York, 2002.

[14] H. Bader, J. Hoigné, Determination of ozone in water by the indigo method, Water Res. 15 (1981) 440-456. https://doi.org/10.1016/0043-1354(81)90054-3

[15] W. Masschelein, M. Denis, R. Ledent, Spectrophotometric determination of residual hydrogen peroxide, Water Sewage Works (1977) 69-72.

[16] J.L. Sotelo, F.J. Beltrán, F.J. Benítez, J. Beltrán-Heredia, Ozone decomposition in water: kinetic study, Ind. Eng. Chem. Res. 26 (1987) 39-43. https://doi.org/10.1021/ie00061a008

[17] B.J. Ershov, P.A. Morozov, The Kinetics of Ozone Decomposition in Water, the Influence of pH and Temperature, Russ. J. Phys. Chem. A 83 (2009) 1295-1299. https://doi.org/10.1134/S0036024409080093

[18] M.E. Lovato, C.A. Martín, A.E. Cassano, A reaction kinetic model for ozone decomposition in aqueous media valid for neutral and acidic pH, Chem. Eng. J. 146 (2009) 486-497. https://doi.org/10.1016/j.cej.2008.11.001

[19] M.O. Buffle, J. Shumacher, S. Meylan, M. Jekel, U. von Gunten, Ozonation and Advanced Oxidation of Wastewater: Effect of O_3 Dose, pH, DOM and $HO^\bullet$. Scavengers on Ozone Decomposition and $HO^\bullet$ Generation, Ozone Sci. Eng. 28 (2006) 247-259. https://doi.org/10.1080/01919510600718825

[20] W.T.M. Audenaert, M. Vandevelde, S.W.H. Van Hulle, I. Nopens, Impact of Dissolved Organic Matter (DOM) on Parameter Sensitivity of a Kinetic Ozone Decomposition Model, Ozone Sci. Eng. 35 (2013) 338-349. https://doi.org/10.1080/01919512.2013.797884

[21] J. Staehelin, J. Hoigné, Decomposition of Ozone in Water in the Presence of Organic Solutes Acting as Promoters and Inhibitors of Radical Chain Reaction, Environ. Sci. Technol. 19 (1985) 1206-1213. https://doi.org/10.1021/es00142a012

[22] J.L. Weeks, J. Rabani, The Pulse Radiolysis of Deaerated Aqueous Carbonate Solutions. I. Transient Optical Spectrum and Mechanism. II. pK for OH Radicals, J. Phys. Chem. 70 (1966) 2100-2106. https://doi.org/10.1021/j100879a005

[23] C.C.D. Yao, W.R. Haag, Rate constants for direct reactions of ozone with several drinking water contaminants, Water Res. 25 (1991) 761-773. https://doi.org/10.1016/0043-1354(91)90155-J

[24] S. Semtisoglou-Tsiapou, M.R. Templeton, N.J.D. Graham, L. Hernández-Leal, B.J. Martijn, A. Royce, J.C. Kruithof, Low pressure UV/H2O2 treatment for the degradation of the pesticides metaldehyde, clopyralid and mecoprop. Kinetics and reaction production formation, Water Res. 91 (2016) 285-294. https://doi.org/10.1016/j.watres.2016.01.017

[25] M.S. Elovitz, U. von Gunten, Hydroxyl radical/ozone ratios during ozonation processes I. The Rct concept, Ozone Sci. Eng. 21 (1999) 239-260. https://doi.org/10.1080/01919519908547239

[26] M.S. Elovitz, U. von Gunten, H.P. Kaiser, Hydroxyl Radical/Ozone Ratios During Ozonation Processes. II. The Effect of Temperature, pH, Alkalinity, and DOM Properties, Ozone Sci. Eng. 22 (2000) 123-150. https://doi.org/10.1080/01919510008547216

[27] J. Staehelin, R.E. Bühler, J, Hoigné, Ozone decomposition in water studied by pulse radiolysis. 2. OH and HO4 as chain intermediates, J. Phys. Chem 88 (1984) 5999-6004. https://doi.org/10.1021/j150668a051

[28] R. Criegee, Mechanism of ozonolysis, Angewandte Chemie International 14 (1975) 745-752. https://doi.org/10.1002/anie.197507451

[29] L.T. Molina, M.J. Molina, Absolute absorption cross sections of ozone in the 185-to-350-nm wavelength range, J. Geophys. Res. 91 (1986) 14501-14508. https://doi.org/10.1029/JD091iD13p14501

[30] W.H. Glaze, J-W- Kang, D-H- Chapin, The chemistry of water treatment processes involving ozone, hydrogen peroxide and ultraviolet radiation, Ozone Sci. Eng. 9 (1987) 335-352. https://doi.org/10.1080/01919518708552148

[31] L. Chu, C. Anastasio, Formation of hydroxyl radical from the photolysis of hydrogen peroxide in ice, J. Phys. Chem. A 109 (2005) 6262-6271. https://doi.org/10.1021/jp051415f

[32] S. Malato, P. Fernández-Ibáñez, M.I. Maldonado, J. Blanco, W. Gernjak, Decontamination and disinfection of water by solar photocatalysis. Recent overview and trends, Catal. Today 147 (2009) 1-59. https://doi.org/10.1016/j.cattod.2009.06.018

[33] M. Qamar, M. Muneer, D. Bahnemann, Heterogeneous photocatalysed degradation of two selected pesticide derivatives, triclopyr and daminozid in aqueous suspensions of titanium dioxide, J. Environ. Manage. 80 (2006) 88-106. https://doi.org/10.1016/j.jenvman.2005.09.002

[34] C. Berberidou, V. Kitsiou, S. Karahanidou, D.A. Lambropoulou, A. Kouras, C.I. Kosma, T.A. Albanis, I. Poulios, Photocatalytic degradation of the herbicide clopyralid: kinetics, degradation pathways and ecotoxicity evaluation, J. Chem. Technol. Biotechnol. 91 (2015) 2510-2518. https://doi.org/10.1002/jctb.4848

[35] G. Xu, N. Liu, M. Wu, T. Bu, M. Zheng, The photodegradation of clopyralid in aqueous solutions: effects of light sources and water constituents, Ind. Eng. Chem. Res. 52 (2013) 9770-9774. https://doi.org/10.1021/ie302844v

[36] D.V. Sojic, V.B. Anderluh, D.Z. Orcic, B. Abramovic, Photodegradation of clopyralid in TiO_2 suspensions: Identification of intermediates and reaction pathways, J. Hazard. Mater. 168 (2009) 94-101. https://doi.org/10.1016/j.jhazmat.2009.01.134

[37] A. Ozcan, Y. Sahin, A.S. Koparal, M. Oturan, Degradation of picloram by electro-Fenton process, J. Hazard. Mater. 153 (2008) 718-727. https://doi.org/10.1016/j.jhazmat.2007.09.015

[38] J. Gomes, R. Costa, R.M. Quinta-Ferreira, R.C. Martins, Application of ozonation for pharmaceuticals and personal care products removal from water, Sci. Total Environ. 586 (2017) 265-283. https://doi.org/10.1016/j.scitotenv.2017.01.216

[39] S. Chiron, A. Fernández-Alba, A. Rodríguez, E. García-Calvo, Pesticide chemical oxidation: state of the art, Water Res. 34 (2000) 366-377. https://doi.org/10.1016/S0043-1354(99)00173-6

[40] J. Nawrocki, J Swietlik, U Raczyk-Stanislawiak, A. Dabrowska, S. Bilozor, W. Ilecki, Influence of Ozonation Conditions on Aldehyde and Carboxylic Acid Formation, Ozone Sci. Eng. 25 (2003) 52-62. https://doi.org/10.1080/713610650

[41] G.A. Gagnon, S.D.J. Booth, S. Peldszus, D. Mutti, F. Smith, P.M. Huck, Carboxylic acids: formation and removal in full-scale plants, J. Am. Water Works Assoc. 89 (1997) 88-97. https://doi.org/10.1002/j.1551-8833.1997.tb08279.x

[42] F.J. Beltrán, A. Rey, Solar or UVA-visible photocatalytic ozonation of water contaminants, Molecules 22 (2017) 1177. https://doi.org/10.3390/molecules22071177